Available online at www.sciencedirect.com

ScienceDirect

journal homepage: www.elsevier.com/locate/issn/15375110

Research Paper

An interactive photogrammetric method for assessing deer antler quality using a parametric Computer-Aided Design system (Interactive Photogrammetric Measure Method)

Miguel A. Rubio-Paramio [a,*], *Juan M. Montalvo-Gil* [a], *José A. Ramírez-Garrido* [b], *Débora Martínez-Salmerón* [c], *Concepción Azorit* [b]

[a] *Department of Engineering Graphics, Design and Projects, University of Jaen, Spain*
[b] *Department of Animal and Vegetal Biology and Ecology, Faculty of Experimental Sciences, University of Jaen, Spain*
[c] *Department of Animal Biology, Faculty of Biology, University of Barcelona, Spain*

ARTICLE INFO

Article history:
Received 30 October 2015
Received in revised form
27 June 2016
Accepted 19 July 2016

Keywords:
Photogrammetry
Parametric 3D modelling
Landmarks
Deer antler
Ecological application
Homologous points

In the area of deer antler evaluation for trophy homologation, as well as in the obtaining of biometric databases for later analysis in the field of Geometric Morphometrics, different linear biometric tools have traditionally been used. In this study we used two sets of antlers from 29 Iberian red deer (*Cervus elaphus hispanicus*) to develop and establish a new photogrammetric technique which creates the 3D model of the antler using a parametric 3D Computer-Aided Design (CAD). This simple and reliable method for deer hunting trophy homologation was compared with the other two more extensively used methods of antler measurement, the traditional measuring tape and the Articulated Arm Coordinate Measuring Machine (AACMM or CMA).

The advantage of this innovative photogrammetric method is the use of only two photographs to obtain both the 3D model and the dimensions required for antler evaluation. A procedure was performed to compare lengths and antler evaluation as hunting trophy. The three methods showed similar reliability, although the photogrammetric process using the 3D CAD system was much faster and more functional than both the traditional measuring tape and Articulated Arm methods. Since this method only requires two photographs per individual, it makes possible the study of a high percentage of antlers in the field.

This new photogrammetric method has been successfully used in the biometrics area, but it could become a more extensively used method in this and other fields because of its ease of operation, speed and accuracy of data collection.

© 2016 IAgrE. Published by Elsevier Ltd. All rights reserved.

* *Corresponding author.*
E-mail address: marubio@ujaen.es (M.A. Rubio-Paramio).
http://dx.doi.org/10.1016/j.biosystemseng.2016.07.012
1537-5110/© 2016 IAgrE. Published by Elsevier Ltd. All rights reserved.

1. Introduction

From the deer hunting point of view there is a growing interest in antler assessment and in their homologation as trophies, as well as in the obtaining of biometric databases for later analysis in the field of Geometric Morphometrics. In order to accomplish this task, new tools and methodologies for facilitating and accelerating the collection and processing of geometric data are necessary. Figure 1 shows the main methods used in the field of biometrics to assess antler quality. Although most tools use both Traditional Measuring and Contact Measuring Methods, new interesting techniques such as 3D Scanner and Photogrammetry have recently been used in Biology, mainly in the field of the creation of 3D Biological models. Furthermore, 3D models can also be measured in order to obtain geometric dimensions. These latest measurement technologies applied to biological elements provide results of high accuracy.

Articulated Arms Coordinate Measuring Machines (AACMM or CMA) are the most common contact measuring instruments used in 3D biological studies for obtaining points coordinates on the surface of the measured element. These articulated arms work based on acquiring the three-dimensional location of landmarks (homologous points located in similar positions on different biological elements) with regard to a reference system. Moreover, the CMA is a highly accurate method, easy to implement in the laboratory. In the field of Geometric Morphometrics it has been used to study especially complex bones of apes and humans, such as for example temporal bones (Harvati, 2003; Lockwood, Lynch, & Kimbel, 2002), mandibles (Nicholson & Harvati, 2006), or craniofacial regions (Kimmerle, Ross, & Slice, 2008).

However, the 3D scanner is currently another technique that performs a highly efficient coordinate digitisation, which is the most accurate in collecting a huge amount of points on the surfaces of the measured elements. It has been used in studies such as biometric and geometric morphometrics (Hennessy & Stringer, 2002), surface acquisition of human body geometry (Fortin et al., 2007) and human shape studies linked to the industry for mannequin creation (Wang, 2005). In fact, industry is the area which uses these techniques more extensively, mainly in the Reverse Engineering field (Korosec, Duhovnik, & Vukasinovic, 2010; Yu & Peng, 2007; Panchetti, Pernot, & Veron, 2010; Beccari, Farella, Liverani, Morigi, & Rucci, 2010), product design and re-design (Goyal et al., 2012; Ye et al., 2008), and building installations (Brilakis et al., 2010, 2011).

Nevertheless, both Scanner 3D and CMA methods are only reproducible in terms of precision in laboratories or controlled environments. This is a drawback of these methods because deer antler studies must usually be carried out outside the laboratory, taking a short time per antler. The data is usually obtained in the field or on a hunting day, the number of specimens is usually high and the conditions are difficult. Both methods are not suitable in the field.

Another interesting method is Photogrammetry. Many studies have used photogrammetry to obtain 3D models similarly to using 3D scanners. This is achieved by generating a large number of photographs of the object, taken from different locations called "viewpoints". A ray is traced from each viewpoint to the points on the object studied. The rays obtained from different viewpoints are intersected in order to produce the three-dimensional coordinates of studied points. By means of the mathematical intersection of converging rays in the space, the precise location of points can be determined.

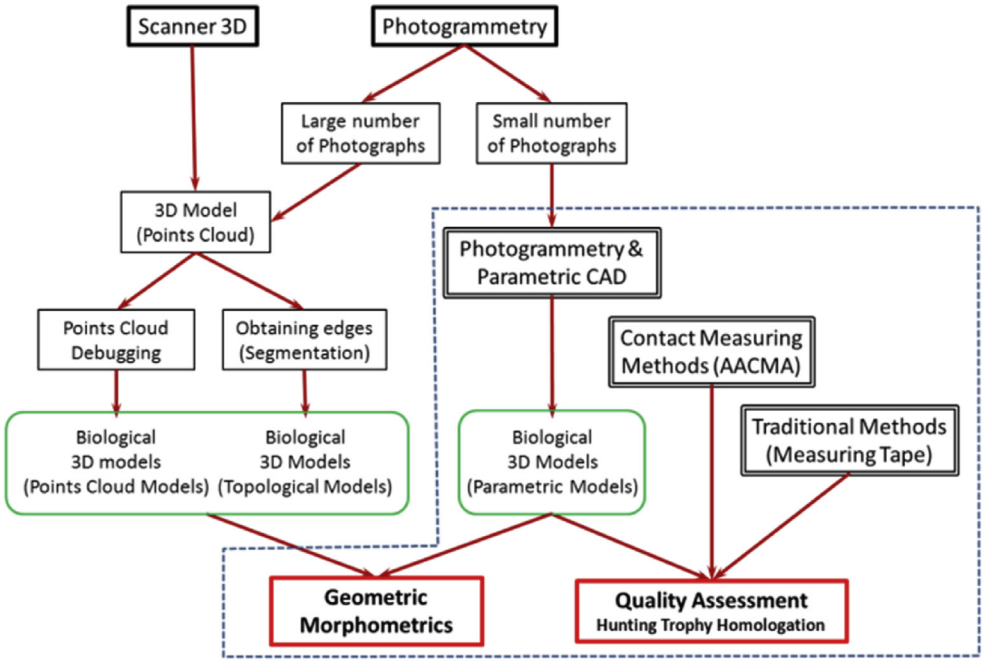

Fig. 1 – The main methods used to obtain 3D models in the field of Geometric Morphometrics and antler quality assessment. We have marked the scope and the methods used in this study.

Some advantages of photogrammetry are its flexibility, low cost and small equipment, and the fact that there is virtually no limit on the size and complexity of the objects measured. Several studies have found that photogrammetry is able to obtain similar results to contact or laser scanning methods in terms of precision, firstly in the field of terrain topography, where photogrammetry was initially applied (Baltsavias, 1999; Liu, Burner, & Jones, 2012), and afterwards for other elements such as buildings (Alves & Bartolo, 2006; Bhatla, Choe, Fierro, & Leite, 2012; Golparvar-Fard, Bohn, Teizer, Savarese, & Peña-Mora, 2011; Ordoñez, Arias, Herraez, Rodriguez, & Martin, 2008), metal structures and ships (Koelman, 2010; Sanchez, Fernandez, Cuesta, Alvarez, & Martinez, 2012; Veldhuis & Vosselman, 1998) and smaller objects (Aguilar, Aguilar, Agüera, & Carvajal, 2005; Ramos & Santos, 2011; Zitova & Flusser, 2003). In the field of medicine it has been used in dental applications (Shigeta et al., 2013).

Usually, the information provided by Photogrammetry consists of clustered points, which reproduce the shape of the elements studied. From clustered points it is possible to create virtual reconstructions of biological elements for different purposes (Chin-Hung, Yun-Sheng, & Wen-Hsing, 2007; Fortin et al., 2007; Shigeta et al., 2013). Due to the large amount of information obtained, data handling may be difficult. This quantity of information necessitates performing a data selection, removing duplicated points as well as the ones located in well-defined areas, and reducing redundant or excess points (Golparvar-Fard et al., 2011; Ramos & Santos, 2011). On the other hand the digitising process is often incomplete, since there are areas which are not captured, resulting in a lack of information on the surfaces obtained. These faults must be corrected later through the use of other techniques. Pernot, Moraru, and Veron (2006) used a mechanical model to simulate curvature variation minimisation. Yan, Yong, Zhang, Paul, and Sun (2006) created an algorithm to fill n-sided holes with NURBS (Non-Uniform Rational B-Splines) patches that interpolate the boundary curves. Wang and Oliveira (2007) presented an algorithm based on moving least squares and interpolated both geometry and shading information. Panchetti et al. 2010 filled these holes by combining the geometric information available on the surrounding area of the holes and the information contained in an image of the real object.

Moreover, the three-dimensional models obtained from photogrammetric or scanned points do not usually provide the exact information needed for the use of biometric and geometric morphometrics techniques. Therefore, from the thousands of points digitised only those consistent with landmarks are needed. The set of landmarks necessary for the geometric study of antlers is small compared with the number of clustered points but, unfortunately, the approximation between digitised points and landmarks is usually low. In order to solve this problem, segmentation techniques based on the identification of significant elements such as edges, vertexes or different sides of the 3D model are used. The results are 3D models of recognisable topology from which landmarks can be extracted (Demarsin, Vanderstraeten, Volodine, & Roose, 2007; Goyal et al., 2012; Wang & Oliveira, 2007; Wu & Yu, 2005; Zitova & Flusser, 2003). In the case of items with irregular shapes, such as some biological structures, additional difficulties could appear.

Recently, several techniques and commercial tools based on the creation of networks of apparent contours have been used to process the photographs. The 3D models obtained are promising, but these are only useful when high accuracy is not required and the objects are not complex (Baumberg, Lyons, & Taylor, 2005; Prakoonwit & Benjamin, 2007; Remondino & El-Hakim, 2006).

Another fact to be taken into account is that the capture of morphological data of antlers requires taking many photographs, but the real situations usually do not allow us to take more than two or three photos per animal. Some authors addressed methods which could reduce the number of photographs. Rodriguez, Martin, Arias, Ordoñez, and Herraez (2008) proposed methods based on taking few photographs to obtain distances measured at different positions. Veldhuis and Vosselman (1998) and Ordoñez et al., 2008 used a reduced number of photographs, based on known geometric restrictions of measured objects, i.e. relationships among straight lines (co-planarity, parallelism, perpendicularity, symmetry and distance). Styliadis (2008) studied the use of only a single image to reconstruct objects.

To obtain the optimal geometric information of real models using a low number of photographs, it is necessary to take into account the geometrical singularities of the models. In our case, the normal morphology of the antler shape is known since it is always based on a trunk with branches. Taking this into consideration, the number of photographs required for generating the 3D models of antlers could be considerably reduced.

Certainly, in practice the most versatile and accurate method of studying antler morphology using a few landmarks and a reduced number of photographs per specimen has been the recreation of the photogrammetric scene of antlers in a 3D Computer-Aided Design (CAD) environment. The CAD 3D modelling technique has been widely used to create human anatomical parts (bio-CAD modelling) and obtain bones and organs for the manufacture of moulds and prototypes (Kurazume et al., 2009; Sun, Starly, Nam, & Darling, 2005), or in the surgical planning and assessment of bone pathologies (Minns, Bibb, Banks, & Sutton, 2003). Fortin et al. (2007) developed a personalised design and adjustment of spinal braces by means of 3D visualisation of the external trunk surface with the underlying 3D bone structures. Parametric CAD models have also been used in the design of body components in order to replace injured elements (Li, Zhang, & Ouyang, 2009). This technology has also been proved useful for the computer modelling of antlers. Specifically, virtual models of real antlers have been successfully created in order to calculate their density, as a substitute to the less practical method based on the Archimedes principle (Paramio et al., 2012).

New procedures can be established to improve obtaining geometric dimensions and the creation of 3D Models by means of parametric CAD systems. The method proposed in the present study develops projective techniques of photogrammetry within a parametric 3D CAD. A virtual parametric three-dimensional scene, crossed by rays, is reproduced. This scene is easily modifiable to a new model because of the parameterisation of the ray-tracing linked to the photographs.

Therefore the main objective of the study has been developing and applying a photogrammetric method, based on parametric 3D CAD technology, which only requires two photographs per individual. The reduced number of photographs allows the study of a high percentage of antlers.

All the methods described above, extensively used to create 3D models, both medium-high cost (optical or laser scanner) and low cost (multi-image photogrammetry and triangulation-based laser scanner) do not allow results to be achieved in the usual scenarios where deer populations are analysed (in days of hunting or in the field, under very difficult conditions and with only a few seconds to obtain the data per specimen). These methods obtain only satisfactory results working with samples in locations in very specific scenarios and very careful conditions such as taxidermy workshops, laboratories, etc.

The new technique proposed in this paper, called the Interactive Photogrammetric Measure Method (IPhMM), has proved a versatile tool for obtaining the needed relevant geometric data instantly (only two photographs are required per specimen) and under unfavourable conditions. Furthermore, later processing does not require a greater time than that needed by other methods. This novel and innovative method is proving to be extremely useful because it allows large populations of deer to be studied with very satisfactory results and the required accuracy.

2. Material and methods

To validate the IPhMM, a sample of an Iberian red deer (*Cervus elaphus hispanicus*) population from the south of Spain was studied in order to obtain a valuable methodology for assessing geometric information from their antlers and the quality of the animals as hunting trophies easily and under field conditions.

2.1. Study area and sample

A sample of two sets of 29 antler trophies from Iberian red deer, of different sizes and tine numbers, collected during the last three hunting seasons in different big game estates in the Sierra Morena (Andalusia, Spain) was used. The first set of 14 antler trophies was measured using the three methods: measuring tape, CMA and IPhMM, while the second set of 15 antler trophies data came from two official homologation sessions and was measured using measuring tape and IPhMM. The measurements were taken by the professional staff of the homologation session.

2.2. Geometric data for antler trophy homologation

Traditionally, trophy homologation has been based on the measurements and score allocation of antlers according to the guidelines described in hunting protocols (I.A.C.P.C., 2015; Llanes, 2013). In the case of the sampled antlers, the following elements were taken into consideration (Fig. 2): the main shaft length, the eye tines length, the trez tines length, the burr perimeter, the perimeters of certain antler points, and the maximum internal separation of antlers. However,

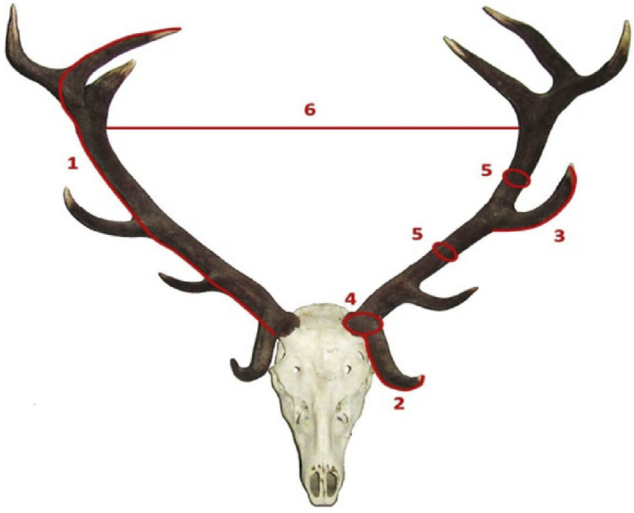

Fig. 2 – Elements to be measured in trophy homologation: 1: Main antler shaft length, 2: Eye tines length, 3: Trez tines length, 4: Burr perimeter, 5: Perimeters of certain antler points. 6: Maximum internal separation of antlers.

there are other quantitative and qualitative antler elements whose valuation is subjective, such as the antler colour, the tine colour and its tip shape, the antler surface roughness (presence of pearls), the total number of tines, the crown length and its number of tines, the bez tines length and the total antler mass.

2.3. Instrumental hardware and software

The corresponding photographs were taken using a handheld PowerShot SX210 IS digital camera, with a resolution of 4320 × 3240 pixels.

The parametric variational CAD system used was SolidWorks by Dassault Systems. A special computer was not required for the processing of the photographs using SolidWorks. However, it was necessary to have a medium-high range graphics card for a better analysis of the photographs. In our case, we used an NVIDIA GeForce GTX 750 1 GB.

Antler measuring was performed using both traditional methods (measuring tape) and an articulated arm coordinate measuring machine (AACMM or CMA) model MicroScribe G2X, with 50″ sphere and 0.009″ (0.23 mm) accuracy.

2.4. Photogrammetric method and CAD-3D technology

Photogrammetry uses photographs as the fundamental means of measurement. From at least two different locations or "lines of sight", the precise location of a point can be determined by means of the mathematical intersection of converging lines in space.

The 3D coordinate determination is based on the point studied, the camera projective centre and the image point lying on a straight line. The determination of the location of a point is obtained through the intersection of two or more straight lines. Therefore, each point should appear in at least two photographs (Fig. 3).

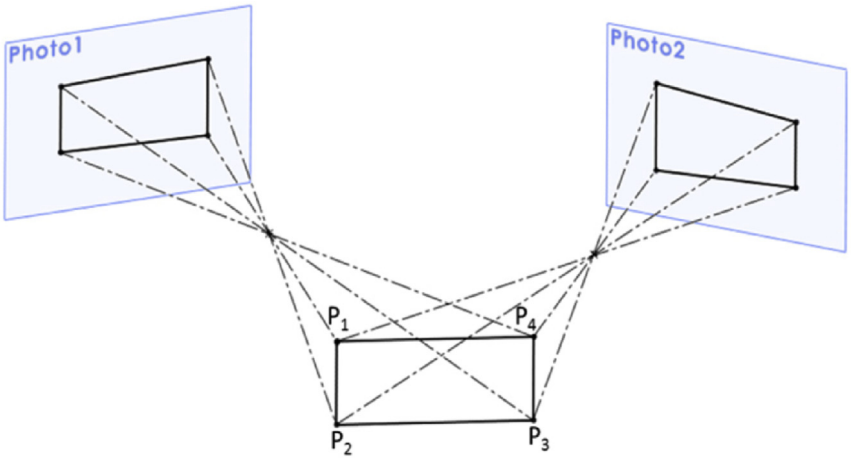

Fig. 3 – Spatial points (P_i) and their rays from two photograph planes (Photo 1, Photo 2).

The relationship between the coordinates of a point, $\mathbf{X_A}$, and those of an image point, $\mathbf{x_a}$, is given by the vector equation

$$\mathbf{X_A} = \mathbf{X_0} - \mu \mathbf{R^t x_a} \quad (1)$$

$\mathbf{X_0}$ are the coordinates of the perspective centre 0 (focus of the camera lens), μ is a scalar and $\mathbf{R^t}$ is the transpose of rotation matrix $\mathbf{R}$, with the elements functions of the camera rotation angles. If the camera position $\mathbf{X_0}$ and the rotation angles are all known, for a single photo there are three equations and four unknowns (μ and the three components of $\mathbf{X_A}$).

This system of equations cannot be resolved, but if there are two cameras, as depicted in Fig. 4, the new system can be resolved because there are now five unknowns (two different values of μ and $\mathbf{X_A}$) and six equations.

However, the camera positions $\mathbf{X_0}$ and the rotation angles are not known in our case and camera position and camera orientation must be treated as unknowns. There are six equations and seventeen unknowns (the three components of $\mathbf{X_A}$, two values of μ, two values of the three components of $\mathbf{X_A}$, and two values of the three components of $\mathbf{X_0}$). Nevertheless, the system of equations becomes over-determined by adding known points. With at least four known points (reference points), the system of equations can be resolved.

The proposed interactive photogrammetric method (IPhMM) consists of the representation of all the ray-tracing of the photograph as a parametric line structure in a three-dimensional virtual CAD environment. To carry it out, two photographs from different perspectives of the structure must be taken in order to allow the location of common points on both of them. This system relies on the fact that on the two photographs identical points (landmarks) are identified.

On the other hand, it is possible to define geometric homologies in the field of the photograph. In the plane of the photograph the real image is reproduced, reduced in scale and inverted (Fig. 5). Successive homological enlargements or reductions of the photograph can be located in parallel planes (Fig. 6). The homology centre is located at the position of the camera lens. However, obtaining non-inverted homologous images of the photograph is also possible. The non-inverted

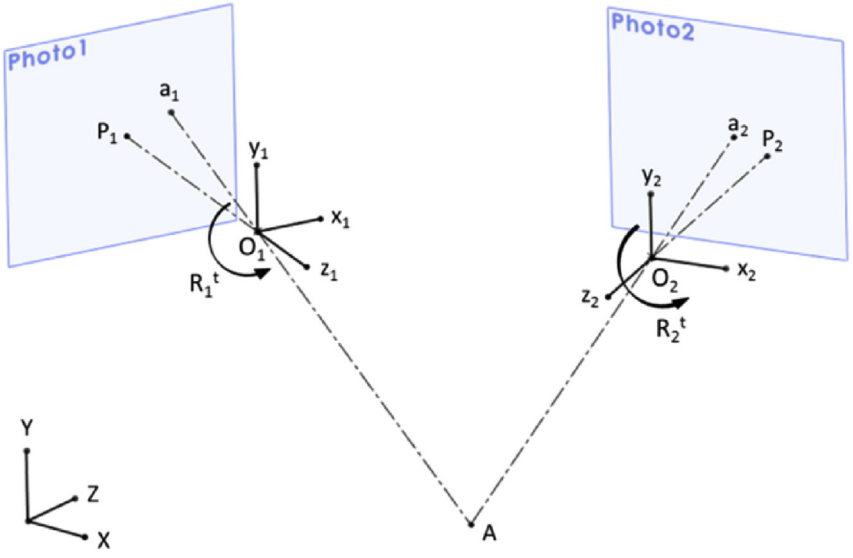

Fig. 4 – Coordinates in the case of two cameras.

Fig. 5 – Trajectory of the rays of incidence on the plane of a photograph. a) Real object; b) position of the camera lens; and c) photograph (reduced in scale and inverted).

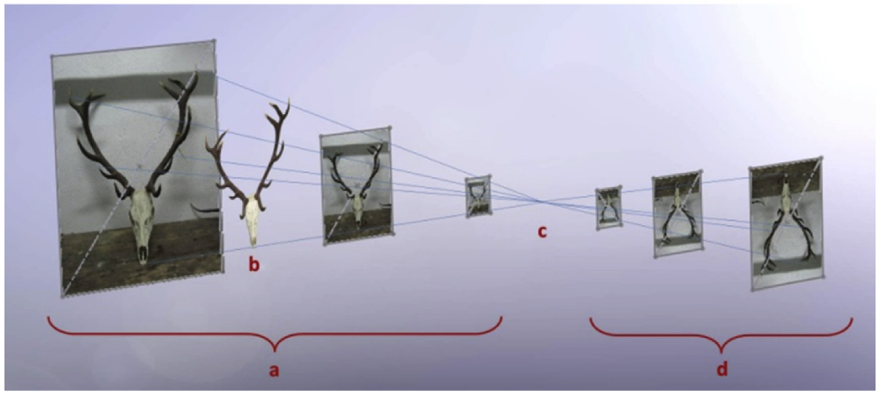

Fig. 6 – Homological images placed in parallel planes, adapted to the rays of a photograph. a) Non-inverted homological images; b) Real object; c) Position of the camera lens (centre of homology); and d) Inverted homological images.

images would appear in planes located between the camera and the real object or behind the real object. We have preferred to use a non-inverted image located behind the real object with a scale factor according to the object size (Fig. 7).

When using the photogrammetric method, it is necessary to include within each photographic scene an item of known geometry and size as a metric reference. In this case a rectangular piece of 594 × 420 mm dimensions, whose four corners needed to appear clearly in the photograph, was used (Fig. 8). These four points will allow us to establish the exact

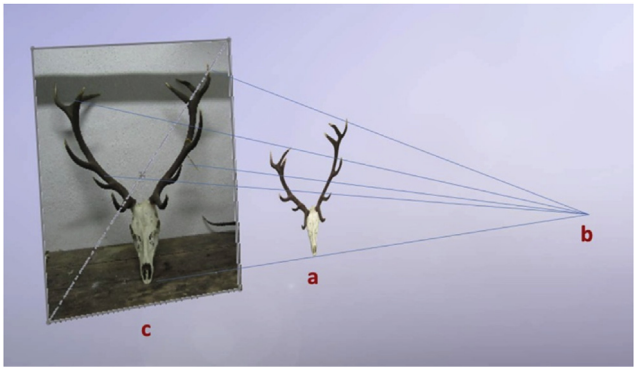

Fig. 7 – The chosen situation in the method. The object (a) is located between the homology centre (b) and a non-inverted photographic image (c). The photographic image will be placed behind the object and be larger than this.

Fig. 8 – Metric reference element of known dimensions behind the antler (rectangular plate of 594 × 420 mm).

position of the viewpoint of each photograph (camera location) as follows:

Inside a virtual scene built in the parametric 3D CAD, a line s perpendicular to the plane of the photograph is traced from the photograph centre (Fig. 9a). This line will end at viewpoint V, origin of the radiation (homology centre) affecting the picture (Fig. 9b). At this time, V is not yet at the correct location along axis s.

A pyramid is built on a polygonal base of four sides, which are included in the photograph plane. Its axis is the line s and its apex is the viewpoint V. Furthermore, the pyramid has four lateral edges that join in the apex of the perpendicular axis described above. The four corners of the pyramid base coincide respectively with the visualisation on the picture of the four corners of the rectangular metric reference used. However, at this time the viewpoint of the photograph or pyramid apex position V has still not been determined and the height of the pyramid is not fixed (Fig. 9b). In order to determine the exact position of the radiation origin, it is necessary to match the lateral edges of the pyramid with the vertices of a rectangle that measures the same as the metric reference (594 × 420 mm). Then, as the CAD system is variational parametric, the apex of the pyramid moves along the perpendicular line s and reaches a fixed position, solving the geometric problem (Fig. 10a). Therefore, the apex position corresponds to the exact location in which the photo was taken, i.e. the camera position. The whole process is repeated for a second photograph by creating a new pyramid linked to the photograph plane. Accordingly, it is possible to obtain the position of a second camera (Fig. 10b).

At this point the same virtual scene is represented from two different points of view with two ray beams departing from each camera position, passing through the real object and affecting the plane of each photograph. Moreover, there is a common element to both ray beams in the space: the rectangular metric reference.

Then a new three-dimensional space where the two radiations affecting the picture match with the two reference elements contained in the lateral edges of the corresponding pyramids is created (Fig. 11a). So a system formed by two projective ray-tracings can fully represent the real scene.

The next step of the process is to match those rays from the two origins of radiation which reach the plane of their corresponding photograph. The point where the ray touches the photograph is matched with a photographed item. The same is done with the ray of the second photograph until it matches with the corresponding photographed element. The point where both rays intersect represents the real position of the item in space (Fig. 11b).

The matchmaking of more rays of light allows real distances to be obtained between visible points of both photographs. An example of this is that a succession of points located on the main antler shaft leads to obtaining both the real position of the curve and its length (Fig. 12a, b and c). The different points are joined by spline curves characterised by adapting to their position, and its length is easily calculated by the system. To measure the antler, the spline passing through a chain of points on the antler surface is drawn. The points are located along the trajectory recommended by the official homologation procedure (I.A.C.P.C., 2015; Llanes, 2013).

Performing this procedure using a variational parametric CAD system allows, in addition, the antlers to be easily modelled in 3D because they are geometrically equivalent.

To obtain the 3D-model, we used the method of volume modelling based on the branched-tree shape of the deer antler developed by Paramio et al. (2012). A set of points are located at the junction points of each branch along the main shaft central spine of the antler. The points are obtained again in the same way by means of the intersection of the two ray-tracings of these points, from the centre of homology to the projection of these points on the plane of each photograph. The central spine of the main shaft is represented by means of a B-spline interpolation curve.

These points describing the central spine are the centres of a set of circles (Fig. 13a). Containing each point of the spine there is located a plane, perpendicular to the spine. A circle at this point on the plane, as a cross-section of the main shaft, is created. To obtain the main shaft, a swept volume passing through all the circles along the spine is modelled (Fig. 13b).

In a second stage, tines are modelled in a similar way. Each tine must be modelled by a new central tine spine passing through three points: at the junction, at the middle and at the tip of the tine. Three cross-sections consisting of three circles are created for each tine. A new swept volume passing through these circles allows the tines to be represented (Fig. 14). A third process smooths the surfaces and bevels the

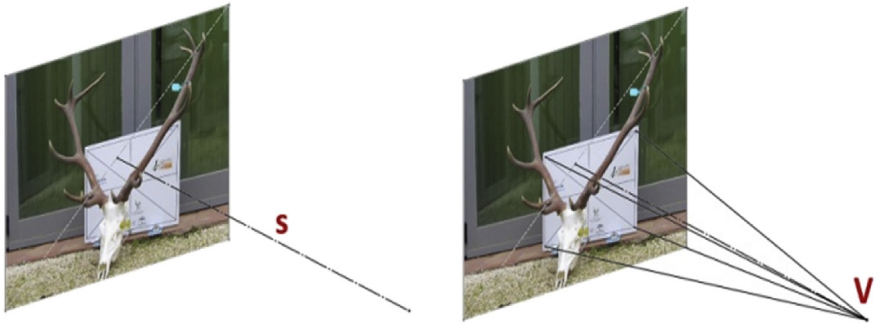

a b

Fig. 9 – a) Creation of the rectangular frame of the photograph and line s perpendicular to the plane of the photograph; b) Pyramidal ray tracing to obtain the centre of homology V.

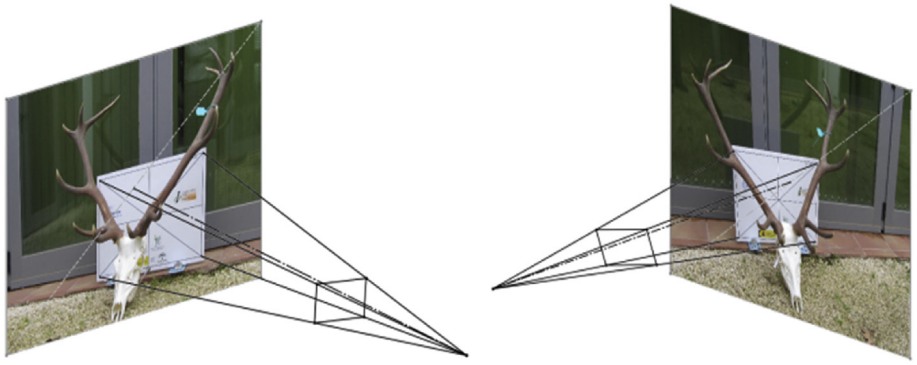

a b

Fig. 10 – Inclusion of the metric reference in true magnitude in the lateral edges of the pyramid. a) Centre of homology of the first photograph; b) Centre of homology of the second photograph.

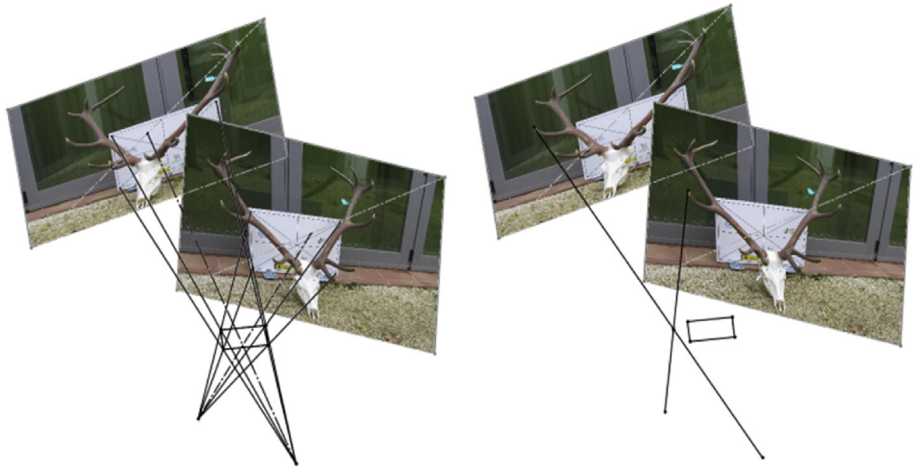

a b

Fig. 11 – a) Matching the two radiations of the reference rectangle viewed on the two photographs. b) Obtaining the spatial location of an element at the intersection of the rays from the element taken on the two photographs.

sharp edges. The modelled branches appear to be more similar to the real ones (Fig. 15a).

The last element of the antler is the burr, the thick ring at the starting zone of the antler. It is modelled by means of a toroid whose centre is the first point of the spine of the main shaft (Fig. 15b). In Fig. 16a, a complete 3D model of the antler is shown. All the geometric elements used to build the 3D model are shown in Fig. 16b.

The set of points necessary to create these geometric elements is accurately located by performing ray-tracing scenery (Fig. 17a). Two rays are intersected to obtain each point (Fig. 17b). The 3D model is built after the set of points is located, following the 3D-model creation process described above (Fig. 17c). A virtual model geometrically equivalent to a real antler is quickly created. Figure 17c shows the 3D model of a cast antler obtained using this method.

To assess the quality of the trophies, it is assumed that the actual perimeters are similar to those of circular sections. The measurements obtained are very close to real ones since the areas where these perimeters are located are far from the tines, where the antlers have almost circular sections. The homologation methodology uses these zones based on this fact (I.A.C.P.C., 2015; Llanes, 2013). For the measurement of the burr, which is the most unfavourable area, the use of the circumference also provides accurate results.

The 3D model and the relevant measurements of the antler can be obtained repeatedly with agility and rapidity by changing the two photographs and fitting the new positions of rays onto the planes of the photographs. The process of obtaining the 3D model takes about 30 min. Obtaining only the measurements of an antler takes about 10–15 min. The photographs were taken in seconds.

We developed the 3D-models taking into account all the usual antler configurations and tine numbers, but special considerations have to be taken into account in relation to defective antlers or those outside the typical morphology.

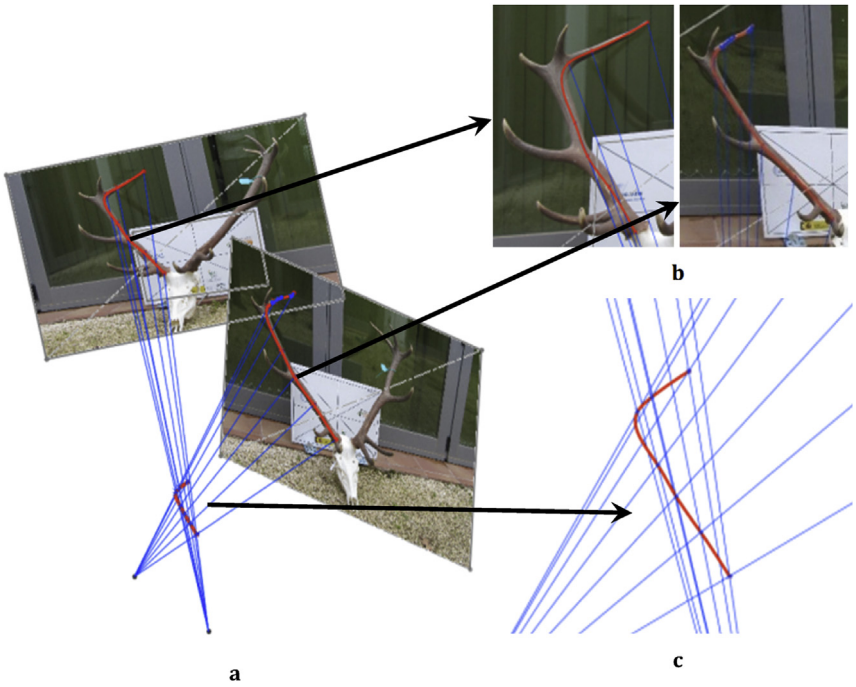

Fig. 12 – Obtaining the real position of a series of points and the line which passes through them. a) Ray-tracing from the two centres of homology of both photographs; b) Locating points of the curves on the photographs; c) The curve in true magnitude is obtained passing through the intersection points of the two ray-tracing.

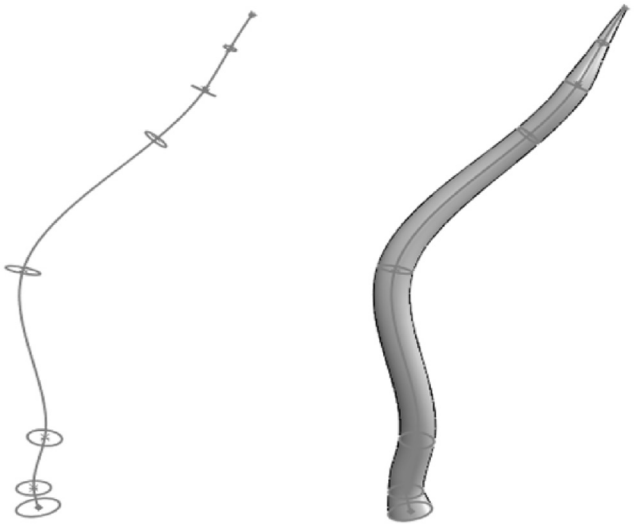

Fig. 13 – a) Central spine of the main shaft antler passing through a set of points. These points are the centres of a set of circles. b) Main shaft of the antler generated by means of a swept volume passing through all the circles.

Certain types of defective or irregular antler that do not match with the developed branched-tree schemes are at the moment not possible to model with this method.

To assess the efficiency of the method, a statistical analysis using Statgraphics Centurion XV v15.2.06 (Stat Point, Inc) was performed. We tested the data normality (Shapiro–Wilk W-test) and homoscedasticity (Levene's test) assumptions and then we assessed differences among methods (lengths calculated by Traditional measuring tape, articulated arm coordinate measuring machine CMA and the proposed photogrammetric CAD method CAD). We used an analysis of variance (ANOVA) and a multiple comparison test. A correlation coefficient was calculated in order to assess the relationship among the lengths obtained by the three methods. Moreover, to provide more information about the individual differences between values from the three methods studied (Tape, CAD and CMA) in the same particular deer, we used a reduced set of 14 deer which were studied using the three different methods. The calculated standard deviation (dv) was used to indicate the variation of the results from the three different methods. We interpreted that lower dv values show the data points tending to be close to the mean, being small enough to be considered in antler quality assessment.

3. Results and discussion

Table 1 shows the statistical comparative results for the first set of 14 antlers (lengths of main shaft, the eye tines, the trez tines, and the maximum internal separation between antler branches) using the three methods (Tape, CAD, CMA), and the comparison of the perimeters at the three positions defined in the homologation process using only two methods, tape and the CAD photogrammetric method (Tape, CAD) because it is not possible to measure perimeters using the CMA method.

There were no significant differences, with a significance level of 0.05, in the lengths using the three methods (the eye

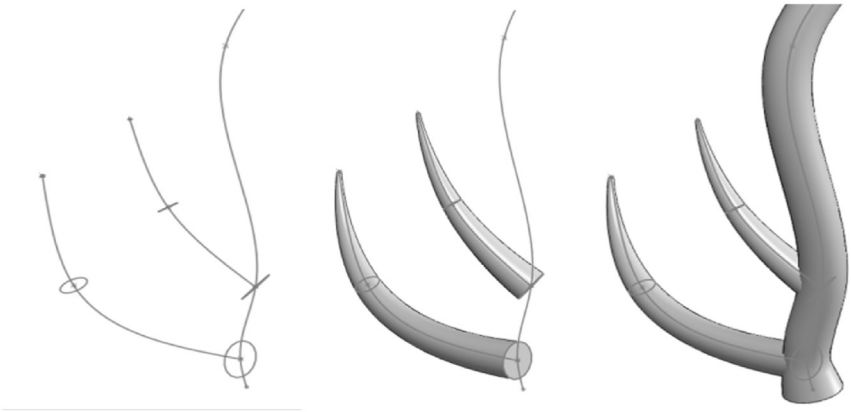

Fig. 14 – Creation of the tines of the antler by means of new spines, circles and swept volumes.

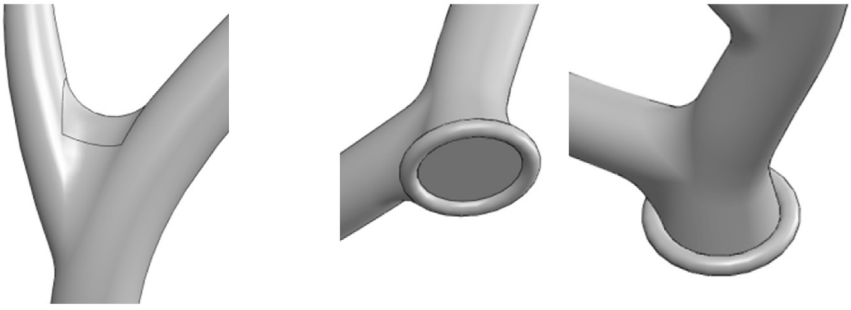

a b

Fig. 15 – a) Smoothing of the surfaces at the starting zone of the tines. b) The burr at starting point of the main shaft.

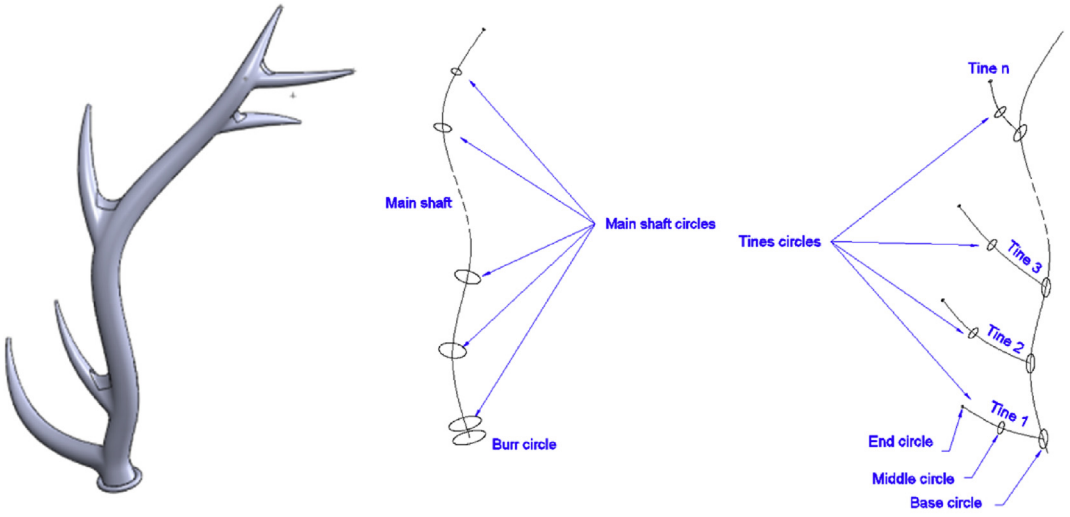

a b c

Fig. 16 – a) Complete 3D model of the antler. b) Main shaft spine and circles. c) Tines spine and circles.

tines P-value = 0.8190, the trez tines P-value = 0.8929 the main shafts P-value = 0.9572 and the maximum internal separation P-value = 0.9877). Perimeters were also not significantly different for the perimeters at the burr, for the perimeters at position 1 and for the perimeters at position 2 (see Table 1).

Table 2 shows the same comparative results for the second set of 15 antlers. In this case only two methods, tape and the CAD photogrammetric method, were used. Tape measuring was carried out by professional operators from an official homologation session whereby the results can be considered more reliable.

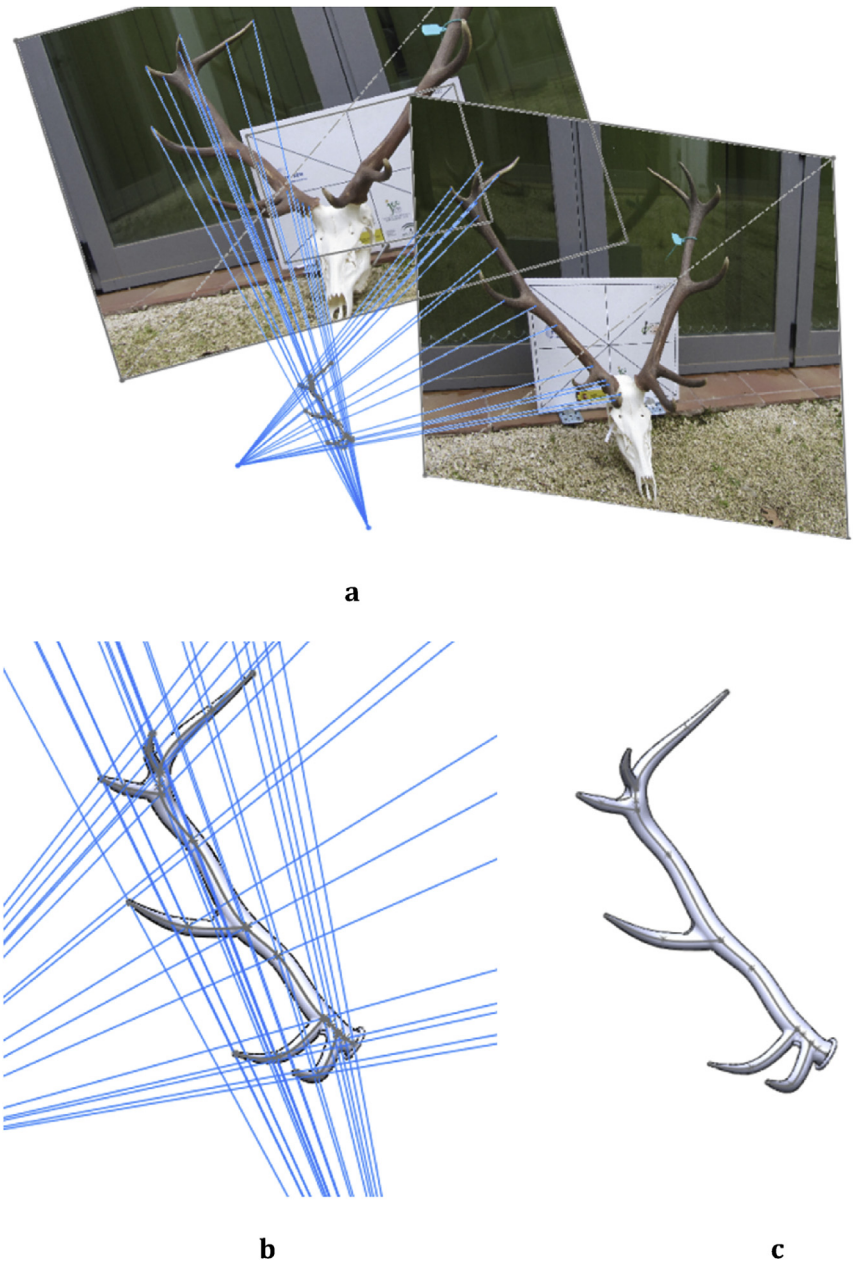

Fig. 17 – a) Ray-tracing scenery to obtain the location of the relevant points for the creation of the 3D model. b) Creation of the 3D model from the set of points. c) 3D model hiding the ray-tracing.

In this second case, there were no significant differences in the lengths of the eye tines, the trez tines, the main shafts or the maximum internal separation as well as for perimeters (the perimeters at the burr at position 1 and at position 2) with a significance level of 0.05 (see Table 2).

The perimeters show greater differences in the second set of antlers because in the process of homologation the operators take the measurement at a point not always located in the middle point of the main shaft between two tines. This way of measuring was used to obtain the highest value for the perimeter.

The results were more similar in the case of greater lengths (main shaft and maximum internal separation). This occurs because in both the CMA and CAD methods the lengths are estimated by curves passing through a set of chosen homologous points. These curves are more adaptable for longer lengths because the number of homologous points is higher. The tines usually have only three or four points but the main shaft could have more than 20. The case of internal separation is more similar because it consists of a straight line.

Table 3 shows a comparative approach of results measuring the differences between the proposed and the conventional methods on each individual separately. Standard deviation (dv) indicates the variation of the three values from the different methods for each deer. We found that dv values lower than 2.5 cm indicate that the data points tend to be close to the mean, being small enough to be considered in antler quality assessment.

Table 1 – Statistical results for the first set of 14 antlers (lengths of eye tines, trez tines, main shafts and max. internal separation, using the three methods -Tape, CAD, CMA-, and perimeters at the three positions defined by the homologation process, using two methods -Tape, CAD).

Element	Number of elements	Method	Length (cm)		ANOVA (P-value)
			Range	Mean ± St. deviation (CV)	
Eye tines	28	CAD	7.43–34.68	21.94 ± 6.57 (29.93%)	F = 0.2; P = 0.82
		CMA	8.17–31.6	22.71 ± 6.04 (26.61%)	
		Tape	6.0–33.0	21.68 ± 6.40 (29.52%)	
Trez tines	28	CAD	8.73–34.94	18.83 ± 6.75 (35.85%)	F = 0.11; P = 0.89
		CMA	8.6–34.9	19.47 ± 6.39 (32.81%)	
		Tape	8.5–35.0	19.61 ± 6.46 (32.94%)	
Main shafts	28	CAD	42.76–85.47	66.35 ± 13.05 (19.67%)	F = 0.04; P = 0.96
		CMA	42.4–86.8	65.75 ± 12.90 (19.62%)	
		Tape	40.0–82.5	65.34 ± 12.84 (19.65%)	
Separation	14	CAD	35.14–77.14	56.98 ± 10.86 (19.05%)	F = 0.01; P = 0.99
		CMA	36.1–79.7	57.16 ± 11.00 (19.25%)	
		Tape	35.5–76.0	56.54 ± 10.49 (18.56%)	
Perimeter at burr	28	CAD	10.73–21.84	16.59 ± 2.67 (16.11%)	F = 0.18; P = 0.68
		Tape	10.5–21.0	16.32 ± 2.27 (13.89%)	
Perimeter at position 1	28	CAD	8.49–13.6	10.97 ± 1.72 (15.72%)	F = 0.05; P = 0.82
		Tape	8.5–14.0	11.07 ± 1.69 (15.29%)	
Perimeter at position 2	28	CAD	7.5–13.09	10.15 ± 1.67 (16.45%)	F = 0.04; P = 0.85
		Tape	8.0–13.0	10.23 ± 1.65 (16.10%)	

Table 2 – Statistical results for the second set of 15 antlers (lengths of eye tines, trez tines, main shafts and max. internal separation, and perimeters at the three positions defined by the homologation process, using two methods -Tape, CAD). In this second case, tape measuring was carried out by professional operators from an official homologation session.

Element	Number of elements	Method	Length (cm)		ANOVA (P-value)
			Range	Mean ± St. deviation (CV)	
Eye tines	30	CAD	19.73–34.06	27.54 ± 3.36 (12.21%)	F = 0.03; P = 0.87
		Tape	21.0–33.7	27.40 ± 3.18 (11.62%)	
Trez tines	30	CAD	19.65–35.85	28.64 ± 4.27 (14.92%)	F = 0.01; P = 0.94
		Tape	19.2–36.6	28.72 ± 4.43 (15.41%)	
Main shafts	30	CAD	75.41–103.69	90.88 ± 7.07 (7.78%)	F = 0.00; P = 0.999
		Tape	74.3–103.1	90.88 ± 6.62 (7.27%)	
Separation	15	CAD	55.95–85.37	73.78 ± 8.67 (11.75%)	F = 0.07; P = 0.79
		Tape	56.0–84.5	72.95 ± 8.23 (11.28)	
Perimeter at burr	30	CAD	17.7–24.3	21.36 ± 1.39 (6.52%)	F = 1.12; P = 0.29
		Tape	17.95–24.89	20.95 ± 1.61 (7.69%)	
Perimeter at position 1	30	CAD	11.2–15.5	12.87 ± 0.97 (7.50%)	F = 3.91; P = 0.05
		Tape	9.61–15.5	12.33 ± 1.16 (9.41%)	
Perimeter at position 2	15	CAD	10.9–14.6	12.28 ± 0.92 (7.50%)	F = 0.11; P = 0.75
		Tape	9.98–15.18	12.19 ± 1.16 (9.53%)	

Antler measurements performed with the Tape method require about 20 min. These measurements must be performed carefully, if possible on a table. The CMA method must preferably be applied in a laboratory, taking about 30–40 min per antler. Finally, the CAD method only needs a few seconds to take the two photographs per specimen. The photo processing takes about 15 min per antler, but this is carried out afterwards using a computer, and far from the field.

The Tape method requires measurements taken by different people, or at least performed by trained people, in order to obtain good results. This is impossible to do in the field or on a hunting day, since the number of specimens is usually high and the conditions are difficult. The CMA method is even more difficult to implement in the field. Taking into account the antler measurements considered by the current trophy homologation protocols, the CMA method would be the least appropriate, since it is not suitable for measuring perimeters.

Our study demonstrates the ability and advantages of this method in the generation of antler morphology. Figure 18a shows the overlapping of the 3D model, and its photographs.

Figure 18b shows the overlapping of the points obtained by means of an articulated arm coordinate measuring machine CMA and the 3D model obtained by means of the proposed IPhMM photogrammetric CAD method. The points obtained by CMA are represented by small white spheres.

4. Conclusions

After the validation of the IPhMM using a collection of antler trophies and obtaining the corresponding parameters, the

Table 3 – Comparative approach of results measuring the differences between the proposed and the conventional methods for each individual separately: dv indicates the standard deviation quantifying the amount of variation for the three values from different methods in each deer. A low dv value indicates that the data points tend to be close to the mean, being small enough to be considered in antler quality assessment.

Deer	Eye tines				Trez tines				Main shafts				Separation			
	Tape	CAD	CMA	dv	Tape	CAD	CMA	dv	Tape	CAD	CMA	dv	Tape	CAD	CMA	dv
1	6.5	7.5	8.73	1.12	12	10.78	11.1	0.63	49	47.55	47.2	0.95	48	48.86	49.1	0.58
2	16	15.49	17.3	0.93	14	16.07	14.2	1.14	40.5	43.14	42.7	1.41	40	39.69	40.2	0.26
3	29	30.01	31.1	1.05	35	34.94	34.9	0.05	82.5	85.47	84.3	1.50	76	77.14	79.7	1.89
4	28	26.46	26	1.05	24	24.01	24.1	0.06	77.5	75.38	75.2	1.28	58	57.41	59.4	1.02
5	21	20.54	22.5	1.02	20	20.09	20	0.05	78	76.05	76.7	0.99	67.5	69.26	68.6	0.89
6	26	26.94	26.3	0.48	20	18.13	20.6	1.29	78.5	79.36	78.8	0.44	60.5	59.09	59.3	0.76
7	33	34.68	31.5	1.59	22	20.3	21.4	0.86	75	76.83	73.2	1.82	61	60.04	60.8	0.51
8	18	17	18.1	0.61	15	13.86	13.6	0.74	57	56.6	55.1	1.00	54.5	54.5	53.6	0.52
9	22	19.22	23.1	2.00	18	16.4	20	1.80	56	58.73	57.4	1.37	50	51.51	50.4	0.78
10	22	22.6	21.6	0.50	23	22.24	21	1.01	60	59.23	60.2	0.51	60	59.71	59.9	0.15
11	20	19.94	21.4	0.83	13	10.95	13	1.18	62.5	62.41	61.5	0.55	58	59.88	59.2	0.95
12	24	24.64	25.2	0.60	21	16.65	19.3	2.19	73.5	75.66	74.9	1.10	61	62.69	62.2	0.87
13	15.5	16.38	16.1	0.45	15.5	15.02	15.4	0.25	55	56.21	54.8	0.76	35.5	35.14	36.1	0.48
14	25.5	23.14	26.5	1.73	25.5	25.43	24.9	0.33	77.5	80.68	77.9	1.73	61.5	62.85	61.7	0.73

a b

Fig. 18 – a) Overlapping the virtual model from the CAD 3D on the real photographed right antler. b) Overlapping of the points obtained by CMA measuring method and the 3D model obtained by means of the IPhMM method.

results were compared with the ones observed through traditional and CMA methods. The three methods showed similar results, providing analogous values for the different antler lengths measured. Differences of size and shape among the antlers sampled were probable, since they showed different morphology conditions.

The Tape and CMA methods are certainly more complex and sometimes more difficult to achieve in the field than the CAD method. Other methods such as optical or laser scanner and triangulation-based laser scanner methods do not allow results to be achieved in the usual scenarios where deer populations are analysed such as on hunting days or in the field, with very difficult conditions and with only a few seconds to obtain the data per specimen. Since the CAD method only requires two photographs per individual, it makes possible the study of a high percentage of antlers in the field. The creation of a 3D photogrammetric scenario within a parametric CAD system allows different pictures to be adapted in a very short time, thereby the later processing of the graphic information with computer assistance is reduced significantly compared with other methods.

On the other hand, since this is a photogrammetric method, it has the advantage of obtaining more interesting information by means of the photographs, whose valuation is somewhat subjective, as for example: the antler colour, the tines shape, the antler surface roughness and so on.

The CAD method has become a useful tool providing data such as lengths, angles, diameters, perimeters, etc. necessary to both trophy homologation and morphometrics analysis. In addition the CAD or IPhMM is a low cost method, which implies low time consumption.

This study has also tried to show the usefulness of the CAD method as an optimal choice in the field of zoological studies, like the ones related to the geometric morphometrics of deer antlers. Additionally, while performing the necessary adjustments, this method could be applied to any anatomical part of any animal species.

Acknowledgements

This study was accomplished by the financial support of the Consejeria de Innovacion Ciencia y Empresa, Junta de Andalucia, the Organismo Autonomo de Parques Nacionales, Ministerio de Medio Ambiente, Medio Rural y Marino, Spain, and the European Fund for Regional Development (FEDER) through grant P07-RNM-03087. The authors wish to thank hunters, guards, farm keepers and taxidermists (Ismael Blanco, Enrique Rodríguez, Fermín Blasco, Jesús Nuñez) for supplying the material necessary for this study.

REFERENCES

Aguilar, M. A., Aguilar, F. J., Agüera, F., & Carvajal, F. (2005). The evaluation of close-range photogrammetry for the modelling of mouldboard plough surfaces. *Biosystems Engineering, 90*(4), 397–407.

Alves, N. M., & Bartolo, P. J. (2006). Integrated computational tools for virtual and physical automatic construction. *Automation in Construction, 15*, 257–271.

Baltsavias, E. P. (1999). A comparison between photogrammetry and laser scanning. *ISPRS Journal of Photogrammetry & Remote Sensing, 54*, 83–94.

Baumberg, A., Lyons, A., & Taylor, R. (2005). 3D S.O.M. commercial software solution to 3D scanning. *Graphical Models, 67*(6), 476–495.

Beccari, C. V., Farella, E., Liverani, A., Morigi, S., & Rucci, M. (2010). A fast interactive reverse-engineering system. *Computer-Aided Design, 42*, 860–873.

Bhatla, A., Choe, S. Y., Fierro, O., & Leite, F. (2012). Evaluation of accuracy of as-built 3D modeling from photos taken by handheld. *Automation in Construction, 28*, 116–127.

Brilakis, I., Fathi, H., & Rashidi, A. (2011). Progressive 3D reconstruction of infrastructure with videogrammetry. *Automation in Construction, 20*, 884–895.

Brilakis, I., Lourakis, M., Sacks, R., Savarese, S., Christodoulou, S., Teizer, J., et al. (2010). Toward automated generation of parametric BIMs based on hybrid video and laser scanning data. *Advanced Engineering Informatics, 24*, 456–465.

Chin-Hung, T., Yun-Sheng, C., & Wen-Hsing, H. (2007). Constructing a 3D trunk model from two images. *Graphical Models, 69*, 33–56.

Demarsin, K., Vanderstraeten, D., Volodine, T., & Roose, D. (2007). Detection of closed sharp edges in point clouds using normal estimation and graph theory. *Computer-Aided Design, 39*(4), 276–283.

Fortin, D., Cheriet, F., Beauséjour, M., Debanné, P., Joncasm, J., & Labelle, H. (2007). A 3D visualization tool for the design and customization of spinal braces. *Computerized Medical Imaging and Graphics, 31*, 614–624.

Golparvar-Fard, M., Bohn, J., Teizer, J., Savarese, S., & Peña-Mora, F. (2011). Evaluation of image-based modeling and laser scanning accuracy for emerging automated performance monitoring techniques. *Automation in Construction, 20*(8), 1143–1155.

Goyal, M., Murugappan, S., Piya, C., Benjamin, W., Fang, Y., Liu, M., et al. (2012). Towards locally and globally shape-aware reverse 3D modeling. *Computer-Aided Design, 44*(6), 537–553.

Harvati, K. (2003). Quantitative analysis of Neanderthal temporal bone morphology using three-dimensional geometric morphometrics. *American Journal of Physical Anthropology, 120*(4), 323–338.

Hennessy, R. J., & Stringer, C. B. (2002). Geometric morphometric study of the regional variation of modern human craniofacial form. *American Journal of Physical Anthropology, 117*(1), 37–48.

I.A.C.P.C. Instituto Andaluz de la Caza y Pesca Continental. (2015). *Reglamento de funcionamiento y manual practico de medicion para la homologacion de trofeos de caza en andalucia*. http://www.juntadeandalucia.es/medioambiente/portaldelacazaylapescacontinental.

Kimmerle, E. H., Ross, A., & Slice, D. (2008). Sexual dimorphism in America: Geometric morphometric analysis of the craniofacial region. *Journal of Forensic Sciences, 53*(1), 54–57.

Koelman, H. J. (2010). Application of a photogrammetry-based system to measure and re-engineer ship hulls and ship parts: An industrial practices-based report. *Computer-Aided Design, 42*, 731–743.

Korosec, M., Duhovnik, J., & Vukasinovic, N. (2010). Identification and optimization of key process parameters in noncontact laser scanning for reverse engineering. *Computer-Aided Design, 42*, 744–748.

Kurazume, R., Nakamura, K., Okada, T., Sato, Y., Sugano, N., Koyama, T., et al. (2009). 3D reconstruction of a femoral shape using a parametric model and two 2D fluoroscopic images. *Computer Vision and Image Understanding, 113*, 202–211.

Liu, T., Burner, A. W., & Jones, T. W. (2012). Photogrammetric techniques for aerospace applications. *Progress in Aerospace Sciences, 54*, 1–58.

Li, N., Zhang, H., & Ouyang, H. (2009). Shape optimization of coronary artery stent based on a parametric model. *Finite Elements in Analysis and Design, 45*, 468–475.

Llanes, L. (2013). *Manual de Homologacion de trofeos de caza mayor en España*. Huelva (Spain): Llanes. ISBN: 978-84-616-5356-0.

Lockwood, C. A., Lynch, J. M., & Kimbel, W. H. (2002). Quantifying temporal bone morphology of great apes and humans: An approach using geometric morphometrics. *Journal of Anathomy, 201*(6), 447–464.

Minns, R. J., Bibb, R., Banks, R., & Sutton, R. A. (2003). The use of a reconstructed three-dimensional solid model from CT to aid the surgical management of a total knee arthroplasty: A case study. *Medical Engineering & Physics, 25*, 523–526.

Nicholson, E., & Harvati, K. (2006). Quantitative analysis of human mandibular shape using three-dimensional geometric morphometrics. *American Journal Of Physical Anthropology, 131*(3), 368–383.

Ordoñez, C., Arias, P., Herraez, J., Rodriguez, J., & Martin, M. T. (2008). Two photogrammetric methods for measuring flat elements. *Automation in Construction, 17*(5), 517–525.

Panchetti, M., Pernot, J. P., & Veron, P. (2010). Towards recovery of complex shapes in meshes using digital images for reverse engineering applications. *Computer-Aided Design, 42*(8), 693–707.

Paramio, M. A. R., Muñoz, J., Moro, J., Gutierrez, R., Oya, A., Tellado, S., et al. (2012). Assessing red deer antlers density with water displacement method versus a new parametric volume modelling technique using CAD-3D. *Animal Production Science, 52*, 750–755.

Pernot, J. P., Moraru, G., & Veron, P. (2006). Filling holes in meshes using a mechanical model to simulate the curvature variation minimization. *Computers & Graphics, 30*, 892–902.

Prakoonwit, S., & Benjamin, R. (2007). 3D surface point and wireframe reconstruction from multiview photographic images. *Image and Vision Computing, 25*, 1509–1518.

Ramos, B., & Santos, E. (2011). Comparative study of different digitization techniques and their accuracy. *Computer-Aided Design, 43*(2), 188–206.

Remondino, F., & El-Hakim, S. (2006). Image-based 3D modeling: A review. *The Photogrammetric Record, 21*(115), 269–291.

Rodriguez, J., Martin, M. T., Arias, P., Ordoñez, C., & Herraez, J. (2008). Flat elements on buildings using close-range

photogrammetry and laser. *Optics and Lasers in Engineering, 46*(7), 541–545.
Sanchez, F., Fernandez, R. I., Cuesta, E., Alvarez, B. J., & Martinez, S. (2012). Study of the technical feasibility of photogrammetry and coordinated measuring arms. *AIP Conference Proceedings, 1431*, 311–318.
Shigeta, Y., Hirabayashi, R., Ikawa, T., Kihara, T., Ando, E., Hirai, S., et al. (2013). Application of photogrammetry for analysis of occlusal contacts. *Journal of Prosthodontic Research, 57*, 122–128.
Styliadis, A. D. (2008). Historical photography-based computer-aided architectural design, demolished buildings information modeling with reverse engineering functionality. *Automation in Construction, 18*(1), 51–69.
Sun, W., Starly, B., Nam, J., & Darling, A. (2005). Bio-CAD modeling and its applications in computer-aided tissue engineering. *Computer-Aided Design, 37*, 1097–1114.
Veldhuis, H., & Vosselman, G. (1998). The 3D reconstruction of straight and curved pipes using digital line. *ISPRS Journal of Photogrammetry and Remote Sensing, 53*(1), 6–16.
Wang, C. C. L. (2005). Parameterization and parametric design of mannequins. *Computer-Aided Design, 37*(1), 83–98.
Wang, J., & Oliveira, M. M. (2007). Filling holes on locally smooth surfaces reconstructed from point clouds. *Image and Vision Computing, 25*, 103–113.
Wu, H., & Yu, Y. (2005). Photogrammetric reconstruction of free-form objects with curvilinear structures. *The Visual Computer, 21*(4), 203–216.
Yan, Y. J., Yong, J. H., Zhang, H., Paul, J. C., & Sun, J. G. (2006). A rational extension of Piegl's method for filling n-sided holes. *Computer-Aided Design, 38*, 1166–1178.
Ye, X., Liu, H., Chen, L., Chen, Z., Pan, X., & Zhang, S. (2008). Reverse innovative design—An integrated product design methodology. *Computer-Aided Design, 40*, 812–827.
Yu, C., & Peng, Q. (2007). A unified-calibration method in FTP-based 3D data acquisition for reverse engineering. *Optics and Lasers in Engineering, 45*, 396–404.
Zitova, B., & Flusser, J. (2003). Image registration methods, a survey. *Image and Vision Computing, 21*, 977–1000.